Nanotechnology **22** (2011) 205704 (7pp) doi:10.1088/0957-4484/22/20/205704

Synthesis and strong optical limiting response of graphite oxide covalently functionalized with gallium phthalocyanine

Yong-Xi Li[1], Jinhui Zhu[1], Yu Chen[1], Jinjuan Zhang[1], Jun Wang[2,3], Bin Zhang[1], Ying He[4] and Werner J Blau[3]

[1] Key Lab for Advanced Materials, Institute of Applied Chemistry, East China University of Science and Technology, 130 Meilong Road, Shanghai 200237, People's Republic of China
[2] Key Lab of Materials for High-Power Laser, Shanghai Institute of Optics and Fine Mechanics, Chinese Academy of Sciences, Shanghai 201800, People's Republic of China
[3] Materials Ireland Polymer Research Centre, School of Physics and the Centre for Research on Adaptive Nanostructures and Nanodevices (CRANN), Trinity College Dublin, University of Dublin, Dublin 2, Ireland
[4] Material Research and Analysis Center, School of Materials Science and Engineering, East China University of Science and Technology, 130 Meilong Road, Shanghai 200237, People's Republic of China

E-mail: chentangyu@yahoo.com and jwang@siom.ac.cn

Received 16 November 2010, in final form 15 February 2011
Published 28 March 2011
Online at stacks.iop.org/Nano/22/205704

Abstract

A soluble graphite oxide (GO) axially substituted gallium phthalocyanine (PcGa) hybrid material (GO–PcGa) was for the first time synthesized by the reaction of $tBu_4PcGaCl$ with GO in anhydrous DMSO at 110 °C in the presence of K_2CO_3. The formation of a Ga–O bond between PcGa and GO has been confirmed by x-ray photoelectron spectroscopy. In contrast to GO, the D and G bands of GO–PcGa in the Raman spectrum are shifted to the lower wavenumbers by $\Delta\nu = 11$ and 18 cm^{-1}, respectively. At the same level of concentration of 0.1 g l^{-1}, GO–PcGa exhibit much larger nonlinear optical extinction coefficients and strong optical limiting performance than GO, $tBu_4PcGaCl$ and C_{60} at both 532 and 1064 nm, implying a remarkable accumulation effect as a result of the covalent link between GO and PcGa. GO–PcGa possesses three main mechanisms for the nonlinear optical response—nonlinear light scattering, two-photon absorption and reverse saturable absorption for the 532 nm pulses and nonlinear light scattering for the 1064 nm pulses. $tBu_4PcGaCl$ does not make any significant contribution to the optical limiting at 1064 nm, while GO–PcGa has a much greater optical limiting response than GO at this wavelength, this suggesting that the PcGa moiety could certainly play an unknown but important role in the GO–PcGa material system.

(Some figures in this article are in colour only in the electronic version)

1. Introduction

Phthalocyanines (Pcs) and their numerous analogs and derivatives are materials of tremendous importance in chemistry, materials science, physics, biology and medicine. A high architectural flexibility in a Pc structure facilitates the tailoring of their physical, optoelectronic and chemical parameters in a very broad range [1–6]. The exploitation of the chemical reactivity of the Ga–Cl bond in the $R_xPcGaCl$ (R: peripheral substituents in the Pc macrocycle) can allow the preparation of a series of highly soluble axially substituted and bridged Pc complexes [7–14]. Axial substituents in

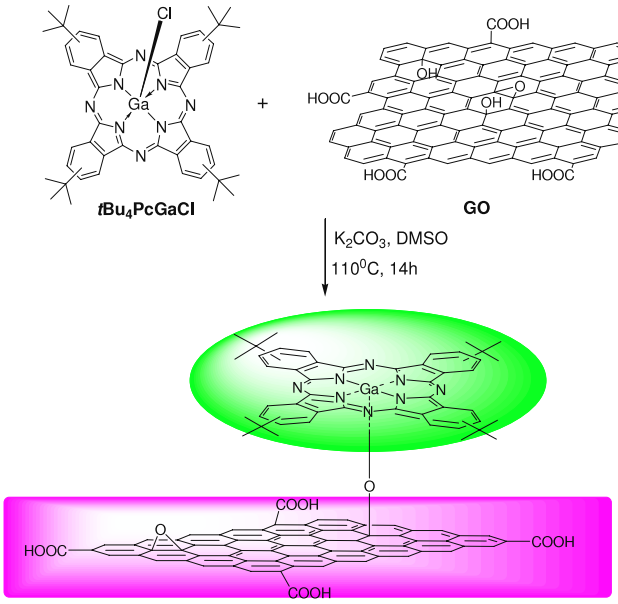

Scheme 1. Synthesis of GO–PcGa.

Pcs influence favorably nonlinear optical (NLO) absorption for the presence of a dipole moment perpendicular to the macrocycle in the axially substituted phthalocyanines [15–21]. Substitution and dimerization of the Pc monomer resulted in significant reductions in the saturation energy density of the material, displaying clear evidence of the usefulness of structurally modifying the phthalocyanine unit. Similar to indium phthalocyanines, gallium phthalocyanines are also one of the most promising materials that have been investigated as limiters of intense light.

Graphene discovered most recently has attracted considerable interest owing to their long-range π-conjugation, yielding extraordinary thermal, mechanical and electrical properties [22–29]. The ultrafast carrier dynamics and large absorption of incident light per layer make graphene a fast saturable absorber over a wide spectral range [30–32]. Wang *et al* [31] observed a significant NLO response of graphene dispersions to nanosecond laser pulses at 532 and 1064 nm, implying a potential broadband optical limiting (OL) application. Nonlinear light scattering (NLS) arising from the formations of solvent bubbles and microplasmas is the principal mechanism for OL. We also observed the NLO and OL properties of graphene families, including graphite oxide (GO; the term 'GO' has been an acronym of graphite oxide for a long time. It should be noted that many papers are using 'GO' for graphene oxide which might be shortened in other ways.) nanosheets, graphene nanosheets (GNSs), GO nanoribbons (GONRs) and graphene nanoribbons (GNRs) at 532 and 1064 nm [32]. GNSs, GONRs and GNRs exhibited broadband NLO and OL properties. NLS and two-photon absorption (TPA) were found to have strong effects on the NLO and OL responses of the graphite nanostructures.

The chemistry of graphene reported in the literature mainly concerns the chemistry of GO [25, 33–35] because GO has chemically reactive oxygen functionality, including carboxylic acid groups and ketone groups at the edges of GO, and epoxy and hydroxyl groups on the basal planes. In our previous work, we synthesized *p*-chlorophenoxygallium(III)2,(3)-tetra-(tert-butyl)phthalocyanine [tBu_4PcGa(*p*-CPO)] by the reaction of tBu_4PcGaCl with *p*-chlorophenol in anhydrous DMSO at 110 °C in the presence of K_2CO_3 [13]. This idea persuaded us to utilize the reactive activity of hydroxyl groups on the basal planes of GO to prepare a first soluble GO axially functionalized gallium phthalocyanine (GO–PcGa) material, as shown in scheme 1. This material displayed excellent strong OL responses at 532 and 1064 nm due to the effective combination of the different NLO mechanisms.

2. Experimental section

2.1. Materials and methods

The operations for synthesis prior to the termination reaction were carried out under purified argon. All chemicals were purchased from Aldrich and used without further purification. Organic solvents were purified, dried and distilled under dry nitrogen. Purified natural graphite was purchased from Shanghai Yifan's Graphite Co. Ltd. tBu_4PcGaCl was synthesized according to the literature reported by us [21].

Fourier transform infrared (FTIR) spectra were recorded on a Nicolet Nagma-IR 550 spectrophotometer using KBr pellets. The ultraviolet/visible (UV/vis) absorption spectral measurements were carried out with a Shimadzu UV-2450 spectrophotometer. Thermal properties of the samples were measured using a Perkin-Elmer Pyris 1 thermogravimetric analyzer in a flowing (100 ml min^{-1}) nitrogen atmosphere. Steady-state fluorescence spectra were measured on a Horiba Jobin Yvon Fluoromax-4 spectrofluorometer. The sample for the fluorescence measurement was dissolved in dry tetrahydrofuran (THF), filtered, transferred to a long quartz cell, and then capped and bubbled with high pure argon (without O_2 and moisture) for at least 15 min before measurement. X-ray photoelectron spectroscopy (XPS) measurements were carried on a Thermo ESCALAB 250 spectrometer with a monochromatized Al Kr x-ray source (1486.6 eV photons) at a constant dwell time of 100 ms and a pass energy of 20 eV. Raman spectra were taken at room temperature with a MicroRaman System RM3000 spectrometer and an argon ion laser operating at a wavelength of 514.5 nm as the excitation source.

To measure the linear and NLO coefficients, GO–PcGa was dispersed in N,N'-dimethylformamide (DMF) at a concentration of 1.0 g l^{-1}, followed by 30 min ultrasonic processing. For the sake of fully evaluating the NLO performance of GO–PcGa, GO, tBu_4PcGaCl as well as C_{60} dispersions were prepared in the same way. All compounds show excellent dispersibility in DMF. As shown in figure 1, the GO dispersions exhibit a brownish color while the GO–PcGa dispersions possess a dark-green color, indicating the existence of the Pc moiety. The solubility of the GO–PcGa is mainly dependent on the percentage of PcGa grafted onto GO.

Linear extinction (absorption and/or scattering) coefficients were measured at a low level of incident light intensity. The linear extinction coefficient, α_0, is defined by $T =$

Figure 1. Digital pictures of the samples dispersed in chloroform: (above) dispersions immediately after sonication; and (bottom) dispersions 1 h after sonication. The concentration for each sample: 1 mg ml^{-1}.

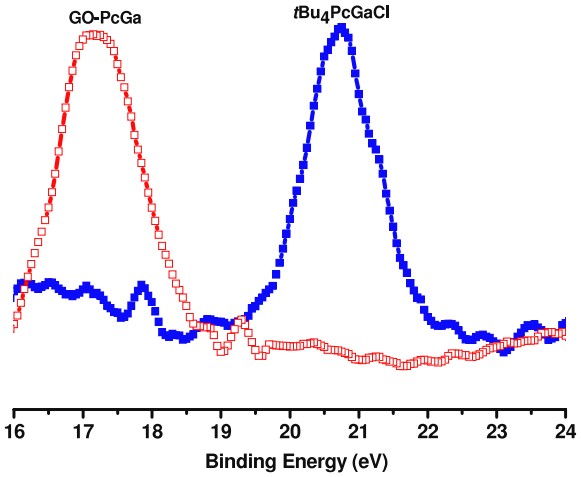

Figure 2. The Ga 3d XPS spectra of the samples.

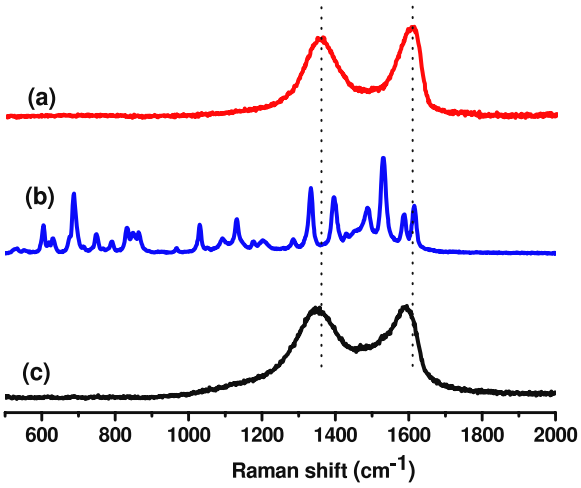

Figure 3. Raman spectra of (a) GO, (b) tBu$_4$PcGaCl and (c) GO–PcGa at 514 nm.

exp($\alpha_0 L$), where T defines the ratio of transmitted to incident laser light and $L = 0.1$ cm is the sample thickness. The NLO properties of the GO–PcGa, GO, PcGaCl and C_{60} dispersions were studied using the open aperture Z-scan technique, which is widely adopted to investigate the nonlinear absorption, scattering and refraction processes. This measures the total transmittance through the material as a function of incident laser intensity, while the sample is gradually moved through the focus of a lens (along the z axis). Effective extinction (absorption and/or scattering) coefficients can be deduced by the theory reported previously [20, 36]. The normalized transmittance as a function of position z, $T_{\text{Norm}}(z)$, is given by $T_{\text{Norm}}(z) = \log[1 + q_0(z)]/q_0(z)$, where $q_0(z) = q_{00}/[1 + (z/z_0)^2]$, z_0 is the diffraction length of the beam. $q_{00} = \beta_{\text{eff}} I_0 L_{\text{eff}}$. β_{eff} is the effective intensity-dependent nonlinear extinction (NLE) coefficient and I_0 is the intensity of the light at focus. L_{eff} is known as the effective length of the sample defined in terms of the linear absorption coefficient, α_0, and the true optical path length through the sample, L, $L_{\text{eff}} = [1 - \exp(-\alpha_0 L)]/\alpha_0$.

In this work, the Z scan was carried out by employing a Q-switched Nd:YAG laser of 6 ns pulses, operated at the fundamental 1064 nm and its second harmonic, 532 nm, with a repetition rate of 10 Hz. The laser beam was tightly focused with a 9 cm focus lens, after spatially removing higher-order modes. Meanwhile, another focusing lens was set up at ∼35° to the direct incident beam to monitor the scattered light from the dispersions. All samples were examined in 0.1 cm quartz cells.

2.2. Preparation of GO

Twelve grams of graphite were suspended in 500 ml of concentrated H_2SO_4 in a 1 l round-bottomed flask under vigorous stirring. Six grams of $KMnO_4$ were then added gradually with stirring and cooling so that the temperature was maintained below 10 °C. The stirring was then continued for 2 h at 35 °C, followed by the addition of 300 ml of deionized water and stirring for another 15 min. Finally the content of the flask was poured into 1 l of deionized water and a sufficient amount of H_2O_2 (50 ml of a 30% aqueous solution) was added to destroy the excess permanganate. Graphite oxide was isolated by centrifugation or filtration through a sintered glass filter, washed with dilute HCl until no sulfates were detected, and then dried for 10 days over P_2O_5 in a vacuum oven before use. 21 g of purified GO was obtained.

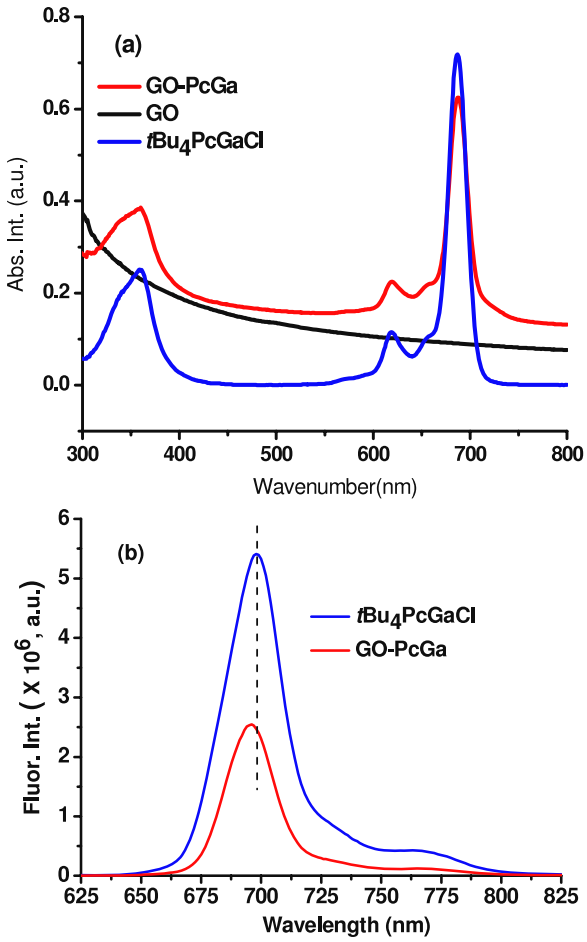

Figure 4. (a) UV/vis absorption and (b) photoluminescence (λ_{ex} = 355 nm) spectra of the samples in DMF.

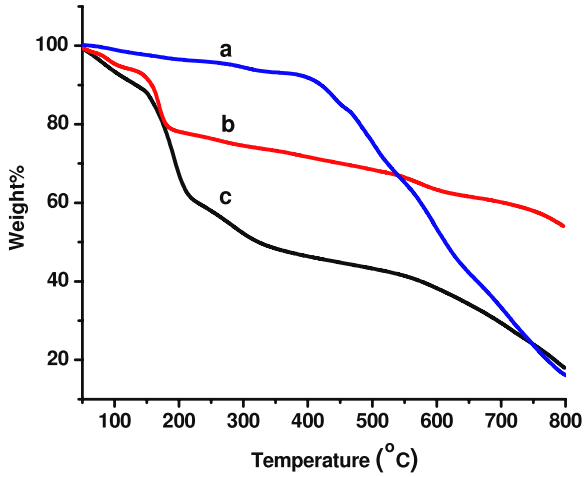

Figure 5. TGA curves of (a) $tBu_4PcGaCl$, (b) GO-PcGa and (c) GO. Heating rate: 10 °C min^{-1}.

2.3. Synthesis of GO–PcGa

To a stirred solution of GO (50 mg) and $tBu_4PcGaCl$[3g] (250 mg) in anhydrous dimethyl sulfoxide (DMSO, 60 ml) was slowly added K_2CO_3 (0.21 g) under purified argon. After refluxing at 110 °C for 14 h, the temperature was allowed to cool to room temperature, while stirring was maintained for a total of 1 h. The mixture was poured into ice water (200 ml) and vacuum-filtered through a single layer nylon film (φ0.22 μm). The black solid on the nylon film was collected, washed with anhydrous Et_2O until the filtrate became colorless and then dried at 60 °C in vacuo for 10 h. Yield: 180 mg. UV/vis ($CHCl_3$): λ (nm^{-1}) = 688, 657(sh), 618, 360; PL (DMF, λ_{ex} = 355 nm): λ_{max} (nm^{-1}) = 696.

3. Results and discussion

The covalent attachment of the PcGa moieties onto the surface of GO was confirmed by XPS, as shown in figure 2. The Ga 3d XPS spectrum of $tBu_4PcGaCl$ shows a peak at 20.8 eV corresponding to the Ga in the Ga–Cl bond. The introduction of GO into the axial position of PcGa resulted in significant blueshift of the peak of gallium functionality relative to $tBu_4PcGaCl$. The peak at 17.2 eV is assigned to the Ga in the Ga–O bond. The Raman spectrum of GO (figure 3, λ_{ex} = 514.5 nm) shows two prominent bands at about 1355 (D band) and 1603 (G band) cm^{-1}. In contrast to GO, the D and G bands of GO–PcGa are shifted to the lower wavenumbers by $\Delta\nu$ = 11 and 18 cm^{-1}, respectively. The D- to G-band intensity ratios (I_D/I_G) increased from 0.88 for Go to 1.01 for GO–PcGa. Usually functionalization of GO and RGO would lead to enhancement of the I_D/I_G ratio because the D band has been used to monitor the process of covalent functionalization which transforms sp^2 to sp^3 sites, while the G band could be utilized to estimate the level and distribution of modification.

The electronic absorption spectra of Pcs are characterized by an intense Q band in the red end of the visible spectrum of light between 600 and 700 nm, and a B band at 300–400 nm in the blue end of the visible spectrum. The influence of different axial substituents on the electronic structure of the phthalocyanine macrocycles is usually very small [7–21, 37–40]. As a result, GO–PcGa displays a linear UV/vis spectrum characterized by a weak redshift of the Q band relative to $tBu_4PcGaCl$ (figure 4). Upon excitation with a 355 nm laser, the photoluminescence spectrum of $tBu_4PcGaCl$ shows a red emission band at λ = 698 nm, while the emission maximum of GO–PcGa is shifted to the blue by $\Delta\lambda$ = 2 nm, followed by a significant decrease of emission intensity when compared to that of $tBu_4PcGaCl$, suggesting that the quenching process is probably due to the electron-transfer process from PcGa to $^1GO^*$.

The thermal properties of GO [41] and GO–PcGa were evaluated by thermogravimetric analysis (TGA). From figure 5. it can be seen that GO is thermally unstable and suffers 15% weight loss upon heating to 100 °C. In agreement with previous reports in the literature for graphene, the main mass loss (~30%) takes place around 200 °C and is ascribed to the decomposition of labile oxygen functional groups present in the material. A ~15% weight loss of GO over the entire temperature range above 300 °C can be attributed to the removal of more stable oxygen functionalities. $tBu_4PcGaCl$ shows good thermal stability, with an onset decomposition temperature of 431 °C. After coupling of PcGa to GO, the

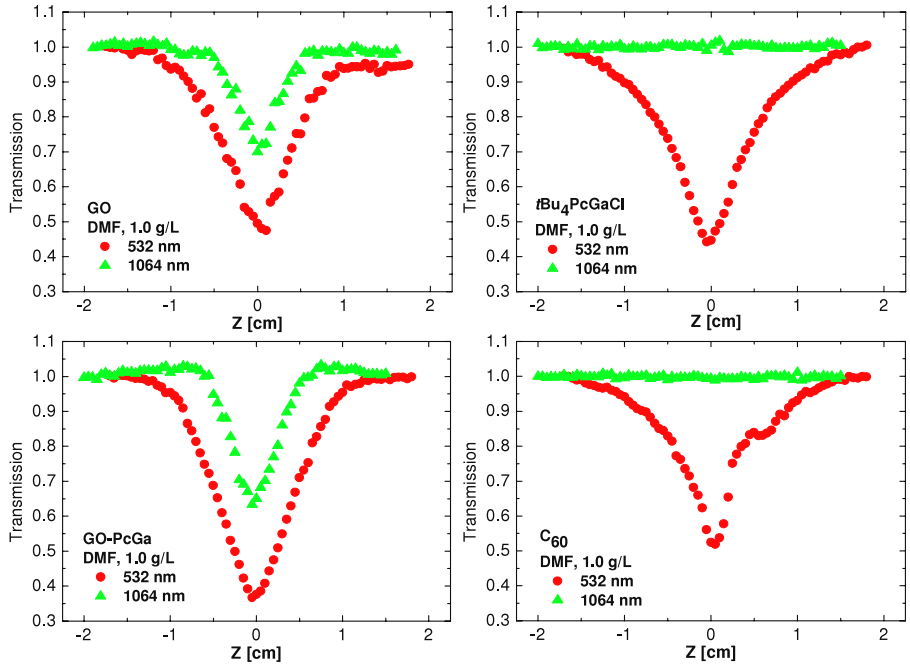

Figure 6. Open aperture Z scans of the samples at 532 and 1064 nm.

Table 1. Linear and NLO coefficients of the samples in DMF at a concentration of 1.0 g l^{-1}. α_0: linear extinction coefficients; β_{eff}: nonlinear extinction coefficient; Im $\{\chi^{(3)}\}$: the imaginary third-order susceptibility.

	532 nm				1064 nm			
Name	T (%)	α_0 (cm^{-1})	β_{eff} (cm GW^{-1})	Im $\{\chi^{(3)}\}$ ($\times 10^{-12}$, esu)	T (%)	α_0 (cm^{-1})	β_{eff} (cm GW^{-1})	Im $\{\chi^{(3)}\}$ ($\times 10^{-12}$, esu)
GO–PcGa	34.3	10.70	67.33 ± 0.63	23.19 ± 0.22	39.7	9.24	11.82 ± 0.38	8.15 ± 0.26
GO	51.9	6.55	28.10 ± 1.41	9.68 ± 0.49	59.9	5.13	6.08 ± 0.78	4.19 ± 0.54
$tBu_4PcGaCl$	87.6	1.33	28.4 ± 0.16	9.79 ± 0.05	93.0	0.72	NA	NA
C_{60}	83.8	1.76	22.57 ± 0.80	8.55 ± 0.30	95.4	0.47	NA	NA

resultant GO–PcGa complex is thermally more stable when compared with GO. When heated to 800 °C, GO–PcGa still retains about 54% of the original mass.

Figure 6 shows the typical open aperture Z-scan data for the GO–PcGa, GO, $tBu_4PcGaCl$ and C_{60}. All Z scans performed at 532 nm exhibited a reduction in the transmission on the focus of the lens, indicating a prominent OL effect. For 1064 nm irradiation both GO–PcGa and GO dispersions show clear NLO responses while $tBu_4PcGaCl$ and C_{60} solutions do not respond at this wavelength. As we have reported previously [31], pristine graphene dispersions exhibit a broadband NLO effect for nanosecond (ns) laser pulses at both 532 and 1064 nm, resulting from the thermally induced NLS. In contrast, the NLO response of GO for ns pulses at 532 nm is attributed to a combination of TPA and NLS [32], in which the latter plays a major role since the TPA is much more pronounced for ps pulses than ns pulses [42, 43]. For the ns pulses at 1064 nm, the NLS dominates the OL response of GO, similar to that of the pristine graphene dispersions. Different from the zero-bandgap graphene, there is a finite bandgap in GO, depending on the functionalization by oxygen-containing groups [44]. Thus, we cannot rule out the possibility of nonlinear absorptions, i.e. multi-photon-absorption and/or excited state absorption of GO at 1064 nm. However, it is expected that the contribution of the nonlinear absorptions to the OL should be minor in comparison with the NLS. $tBu_4PcGaCl$ and C_{60} solutions have large reverse saturable absorption (RSA) at 532 nm but being incapable of absorbing nonlinearly at 1064 nm [7]. From the above analysis, it is credible that GO–PcGa possesses three main mechanisms for the NLO response—NLS, TPA and RSA for the 532 nm pulses and NLS for the 1064 nm pulses. The Z scans of GO–PcGa have a much deeper reduction in transmission than those of GO at the same level of incident fluence, indicating a stronger NLO response. In addition to the contribution of the GO moiety, the PcGa manifests its contribution in the enhanced NLO response at 532 nm due to RSA. Table 1 summarizes the linear and NLO coefficients of GO–PcGa, GO, $tBu_4PcGaCl$ and C_{60}, where the nonlinear extinction coefficients β_{eff} were deduced from the Z-scan fitting. At the same level of concentration of 0.1 g l^{-1}, of all the four materials, GO–PcGa exhibits the largest linear absorption coefficient, nonlinear extinction coefficient and imaginary third-order susceptibility at both 532 and 1064 nm, implying a remarkable accumulation effect as a result of the covalent link between GO and PcGa.

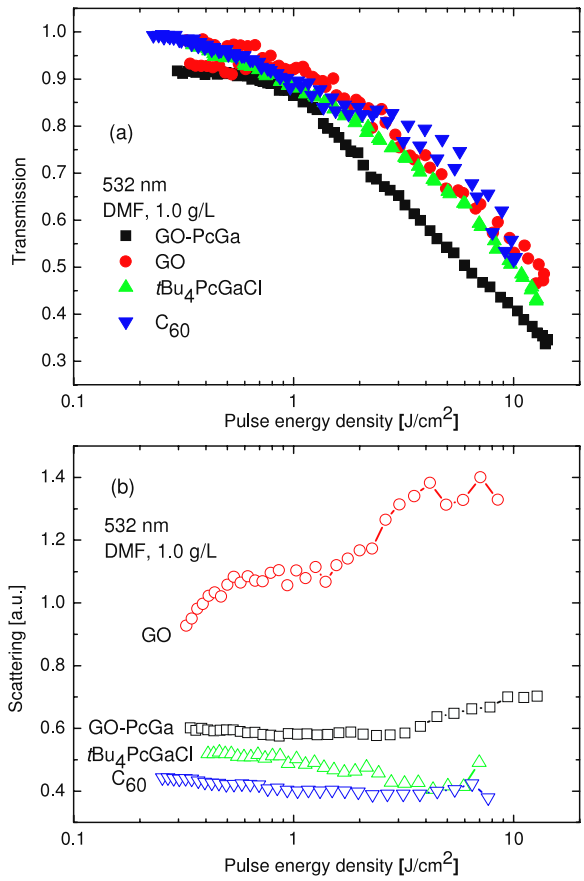

Figure 7. Nonlinear transmission (a) and scattering (b) of the samples at 532 nm.

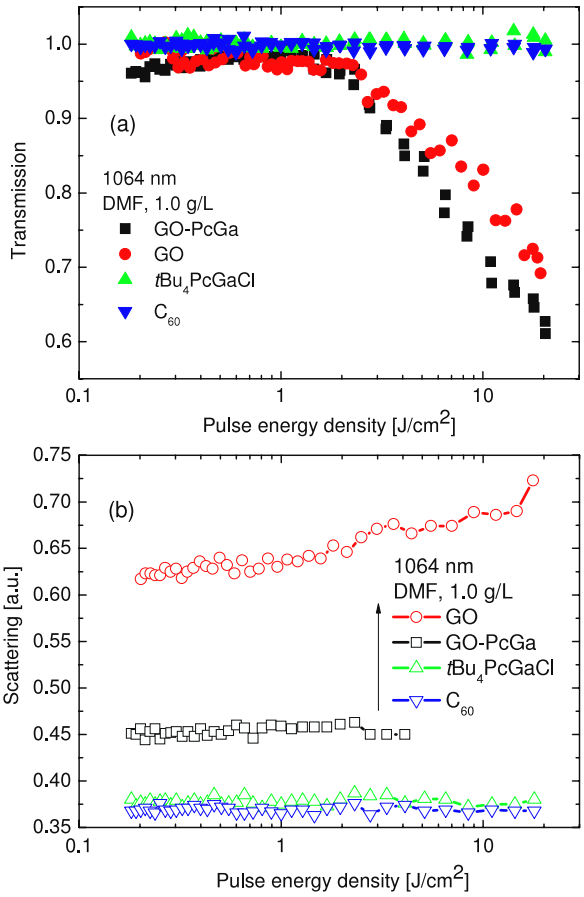

Figure 8. Nonlinear transmission (a) and scattering (b) of the samples at 1064 nm.

Figure 7, in which the normalized transmission and the corresponding scattering were plotted as functions of input energy density (J cm^{-2}), presents the OL performance of the samples at 532 nm. At the same level of concentration, GO–PcGa possesses much better OL performance than the other three materials. The enhanced OL response at 532 nm can be attributed to the effective combination of the different OL mechanisms, i.e. RSA in $tBu_4PcGaCl$ and NLS and TPA in GO. As shown in figure 7(b), significant light scattering signals were observed from GO–PcGa and GO. No scattering was seen from $tBu_4PcGaCl$ and C_{60}, where only RSA dominates at 532 nm.

Figure 8(a) shows the OL performance of the four materials at 1064 nm. As expected, $tBu_4PcGaCl$ does not make any significant contribution to the OL at 1064 nm, while GO–PcGa has a much greater OL response than GO. On the other hand, it is seen in figure 8(b) that the scattered light from GO–PcGa is much weaker than that from GO, which is explainable as the number density of the GO moiety in GO–PcGa should be smaller than that in the pristine GO dispersions. Therefore it is difficult to explain why GO–PcGa is superior to GO for OL if we consider the NLS as the only mechanism. The PcGa moiety could certainly play an unknown but important role in the GO–PcGa material system. Although the origin of such an improvement of the OL at 1064 nm is not clear yet, it is undoubted that GO–PcGa has much better broadband NLO and OL performance than GO or $tBu_4PcGaCl$ alone.

In summary, a soluble graphite oxide axially substituted gallium phthalocyanine hybrid material was synthesized. At the same level of concentration, GO–PcGa exhibits much larger NLO extinction coefficients and strong OL performance than GO, $tBu_4PcGaCl$ and C_{60} at both 532 and 1064 nm, implying a remarkable accumulation effect as a result of the covalent link between GO and PcGa.

Acknowledgments

The authors are grateful for the financial support of the National Natural Science Foundation of China (20676034 and 20876046), the Ministry of Education of China (309013), the Fundamental Research Funds for the Central Universities, the Shanghai Municipal Educational Commission for the Shuguang Fellowship (08GG10) and the Shanghai Eastern Scholarship.

References

[1] Nalwa H S and Shirk J S in 1996 *Phthalocyanines: Properties and Applications* vol 4, ed C C Leznoff and A B P Lever (New York: VCH) p 83

[2] Hanack M and Lang M 1994 *Adv. Mater.* **6** 819–33

[3] Mckeown N B 1998 *Phthalocyanine Materials: Synthesis, Structure and Function* ed B Dunn, J W Goodby and A R West (Cambridge: Cambridge University Press)
[4] De La Torre G, Vazquez P, Agullo-Lopez F and Torres T 1998 *J. Mater. Chem.* **8** 1671–83
[5] De La Torre G, Vazquez P, Agullo-Lopez F and Torres T 2004 *Chem. Rev.* **104** 3723–50
[6] Nemykin V N and Lukyanets E A 2010 *ARKIVOC* 136–208
[7] Chen Y, Hanack M, Araki Y and Ito O 2005 *Chem. Soc. Rev.* **34** 517–29
[8] Chen Y, Fujitsuka M, O'Flaherty S M, Hanack M, Ito O and Blau W J 2003 *Adv. Mater.* **15** 899–902
[9] Chen Y, O'Flaherty S, Fujitsuka M, Hanack M, Subramanian L R, Ito O and Blau W J 2002 *Chem. Mater.* **14** 5163–8
[10] Chen Y, Subramanian L R, Fujitsuka M, Ito O, O'Flaherty S M, Blau W J, Schneider T, Dini D and Hanack M 2002 *Chem. Eur. J.* **8** 4248–54
[11] Claessens C G, Gouloumis A, Barthel M, Chen Y, Martin G, Agullo-Lopez F, Ledoux-Rak I, Zyss J, Hanack M and Torres T 2003 *J. Porphyr. Phthalocya.* **7** 291–5
[12] Yang G Y, Hanack M, Lee Y W, Chen Y, Yuen M L K, Vagin S and Dini D 2003 *Chem. Eur. J.* **9** 2758–62
[13] Chen Y, O'Flaherty S M, Hanack M and Blau W J 2003 *J. Mater. Chem.* **13** 2405–8
[14] Bertagnolli H, Blau W J, Chen Y, Dini D, Feth M P, O'Flaherty S M, Hanack M and Krishnan V 2005 *J. Mater. Chem.* **15** 683–9
[15] Chen Y, Hanack M, Blau W J, Dini D, Doyle J, Liu Y, Lin Y and Bai J 2006 *J. Mater. Sci.* **41** 2169–85
[16] Chen Y, EI-Khouly M E, Sasaki M, Araki Y and Ito O 2005 *Org. Lett.* **7** 1613–6
[17] Chen Y, EI-Khouly M E, Doyle J J, Lin Y, Liu Y, Notaras E, Blau W J and O'Flaherty S M 2008 *Handbook of Organic Electronics and Photonics* vol 2 (Stevenson Ranch, CA: American Scientific Publishers) pp 151–81
[18] Chen Y, Barthel M, Seiler M, Subramanian L R, Bertagnolli H and Hanack M 2002 *Angew Chem. Int. Eng. Edn* **41** 3239–42
[19] Chen Y, Dini D, Hanack M, Fujitsuka M and Ito O 2004 *Chem. Commun.* 340–1
[20] O'Flaherty S M, Hold S V, Cook M J, Torres T, Chen Y, Hanack M and Blau W J 2003 *Adv. Mater.* **15** 19–32
[21] Chen Y, Subramanian L R, Barthel M and Hanack M 2002 *Eur. J. Inorg. Chem.* 1032–4
[22] Wu J, Pisula W and Muellen K 2007 *Chem. Rev.* **107** 718–47
[23] Chen F and Tao N J 2009 *Acc. Chem. Res.* **42** 429–38
[24] Dreyer D R, Park S, Bielawski C W and Ruoff R S 2010 *Chem. Soc. Rev.* **39** 228–40
[25] Park S and Ruoff R S 2009 *Nat. Nanotechnol.* **4** 217–24
[26] Rao C N R, Sood A K, Subrahmanyam K S and Govindaraj A 2009 *Angew. Chem. Int. Edn* **48** 7752–77
[27] Lee C, Wei X, Kysar J W and Hone J 2008 *Science* **321** 385–8
[28] Stoller M D, Park S, Zhu Y, An J and Ruoff R S 2008 *Nano Lett.* **8** 3498–502
[29] Zhang Y, Tan Y W, Stormer H L and Kim P 2005 *Nature* **438** 201–4
[30] Sun Z, Hasan T, Torrisi F, Popa D, Privitera G, Wang F, Bonaccorso F, Basko D M and Ferrari A C 2010 *ACS Nano* **4** 803–10
[31] Wang J, Hernandez Y, Lotya M, Coleman J N and Blau W J 2009 *Adv. Mater.* **21** 2430–5
[32] Feng M, Zhan H and Chen Y 2010 *Appl. Phys. Lett.* **96** 033107
[33] Loh K P, Bao Q, Ang P K and Yang J 2010 *J. Mater. Chem.* **20** 2277–89
[34] Zhuang X D, Chen Y, Liu G, Li P P, Zhu C X, Kang E T, Noeh K G, Zhang B, Zhu J H and Li Y X 2010 *Adv. Mater.* **22** 1731–5
[35] Zhang B, Chen Y, Zhuang X D, Liu G, Yu B, Kang E T and Li Y X 2010 *J. Polym. Sci.* A **48** 2642–9
[36] Sheikbahae M, Said A A, Wei T H, Hagan D J and Vanstryland E W 1990 *IEEE J. Quantum Electron.* **26** 760–9
[37] Hanack M, Schneider T, Barthel M, Shirk J S, Flom S R and Pong R G S 2001 *Coord. Chem. Rev.* **219–221** 235–58
[38] Shirk J S, Pong R G S, Flom S R, Heckmann H and Hanack M 2000 *J. Phys. Chem.* A **104** 1438–49
[39] Perry J W *et al* 1996 *Science* **273** 1533–6
[40] Barthel M, Vagin S, Dini D and Hanack M 2002 *Eur. J. Org. Chem.* 3756–62
[41] Georgakilas V, Bourlinos A B, Zboril R, Steriotis T A, Dallas P, Stuboscd A K and Trapalisa C 2010 *Chem. Commun.* **46** 1766–8
Becerril H A, Mao J, Liu Z, Stoltenberg R M, Bao Z and Chen Y 2008 *ACS Nano* **2** 463–70
Paredes J I, Villar-Rodil S, Martínez-Alonso A and Tascón J M D 2008 *Langmuir* **24** 10560–4
Li P P, Chen Y, Zhu J, Feng M, Zhuang X, Lin Y and Zhan H 2011 *Chem. Eur. J.* **17** 780–5
[42] Wang J and Blau W J 2009 *J. Opt. A: Pure Appl. Opt.* **11** 024001
[43] Liu Z B, Wang Y, Zhang X L, Xu Y F, Chen Y S and Tian J G 2009 *Appl. Phys. Lett.* **94** 02192
[44] Boukhvalov D W and Katsnelson M I 2008 *J. Am. Chem. Soc.* **130** 10697–701